Multiple Collimated Outflows in the Proto-planetary Nebula GL 618

Susan R. Trammell
Physics Department, University of North Carolina at Charlotte, Charlotte, NC 28223
and

Robert W. Goodrich
The W. M. Keck Observatory, 65-1120 Mamalahoa Highway, Kamuela, HI 96743

ABSTRACT

We present narrow-band Hα, [S II], and [O I] Hubble Space Telescope images of the young planetary nebula GL 618. This object is a compact, bipolar nebula that is currently undergoing the transition from asymptotic giant branch star to planetary nebula. Our images confirm the presence of at least three highly collimated outflows emanating from the central regions of GL 618. We also detect Hα emission close to the central dust lane and in an extended scattered light halo. The three outflows are occurring simultaneously in this object, as opposed to being the result of a precessing jet. We derive an inclination for the brightest outflow in the East lobe of $39^{\circ}\pm 4^{\circ}$. This differs from the previous estimate of 45°. In addition, our results indicate that the outflows seen in GL 618 are probably not coplanar. Line strengths derived from the narrow-band images indicate a shock velocity in the range of $40 - 100$ km s^{-1}. Based on the shock velocity we estimate that the age of the outflows is less than 500 years. The outflows seen in the optical images of GL 618 are related to features seen in near-IR, CO and CS maps of this object. This relationship indicates that the outflows are playing a major role in the morphological evolution of this young planetary nebula, interacting with and shaping the neutral envelope surrounding GL 618. We discuss the implications of these jets and their interaction with the neutral envelope in the context of current models of planetary nebula formation.

Subject headings: circumstellar matter—ISM: jets and outflows—planetary nebulae: general—planetary nebulae: individual(GL 618)

1. Introduction

Kwok, Purton, and Fitzgerald (1978) introduced the interacting winds model to account for the development of spherical planetary nebulae (PN). In this model a massive, low-velocity wind removes a large fraction of the envelope material during the asymptotic giant branch (AGB) phase of evolution, and is followed by a higher-velocity, lower-mass wind. The high-velocity wind snowplows into the previously ejected AGB wind material and sweeps up gas to form a PN. The majority of PN exhibit aspherical structure, ranging from slightly elliptical to bipolar (Greig 1971; Zuckerman and Aller 1986; Balick 1987; Schwarz, Corradi, and Melnick 1992; Manchado et al. 1996). Other investigators have extended the interacting winds model to explain the formation of these aspherical objects (Khan and West 1985; Balick 1987; Soker and Livio 1989; Icke, Balick, and Frank 1992; Frank 1994; Dwarkadas, Chevalier, and Blondin 1996).

Understanding the origin of asymmetric structure in PN has been the focus of extensive research in recent years. To achieve asymmetric PN morphologies, the interacting winds model requires that mass loss during the early phases of the de-

velopment of these objects is aspherical. This aspherical structure is then amplified through the wind-shaping that occurs as the PN evolves. Observationally, the time that aspherical structure becomes important is becoming clear. Mass loss during the AGB is predominantly spherical (Neri et al. 1998; Meixner et al. 1998), while the morphologies of proto-planetary nebulae are typically aspherical (Trammell, Dinerstein, and Goodrich 1994; Meixner et al. 1997; Dayal et al. 1998; Kwok, Su, and Hrivnak 1998; Ueta, Meixner, and Bobrowsky 2000). These findings indicate that during the late-AGB and/or post-AGB phase, the mass loss becomes aspherical (Kastner, Soker, and Rappaport 2000, for reviews). The mechanism that triggers this change in the character of the mass loss is not well understood. Suggestions for this trigger range from binary star evolution (Morris 1981; Soker and Livio 1994) to the effects of magnetic fields (Garcia-Sergura 1997).

A recent HST narrow-band Hα survey of the morphologies of low excitation PN (Sahai and Trauger 1998a) revealed a dazzling array of complex structures in these objects including jets, knots, bubbles, and loops. The large variety of structures seen in these images cannot be explained by the interacting winds model alone. Sahai & Trauger suggested that phenomena such as jets acting during the early post-AGB phase may play a role in creating the complex structures seen in these objects. Recent CO observations of several young PN with collimated outflows have demonstrated that these outflows are significantly disrupting and interacting with the neutral shells surrounding these objects (Forveille et al. 1998; Cox et al. 2000; Huggins et al. 2000; Bachiller et al. 2000). Both the HST imaging and the CO observations suggest that jets could have a significant impact on the way we think about the evolution of PN. The interaction of the jet with previously ejected material may influence the morphological evolution of PN in a way that is not considered in current models of PN formation. Further, the phenomena driving the change from spherical to aspherical mass loss in the early stages of PN development are not clear. The formation of jets may play a role in the change to aspherical mass loss in some objects.

If jets are playing a major role in the shaping of PN, their influence will be most significant at a time when the PN still has a large neutral envelope and before the fast wind develops. We present HST observations of GL 618, a young PN undergoing the stage of evolution immediately preceding the PN phase, during which recently lost material has begun to disperse but the fast wind has not fully developed. GL 618 is surrounded by a shell of dust and neutral gas that extends well beyond the optical nebula (Speck, Meixner, and Knapp 2000; Meixner et al. 1998, and references therein). Our new observations have allowed us to confirm that jets are present in GL 618 and to better understand the importance of these outflows in development of this object.

Ground-based optical and near-IR imaging of GL 618 reveal two lobes of emission (each about $3''$ in extent) separated by a dark lane. The central regions of the nebula are hidden from direct view at optical and near-IR wavelengths by the lane of obscuring material. The spectrum of GL 618 is composed of a faint continuum and a variety of low-excitation emission lines. Schmidt and Cohen (1981) and Trammell, Dinerstein, and Goodrich (1993) used spectropolarimetry to study GL 618 and found that the continuum and part of the permitted line emission are reflected from deep in the nebula. The low-excitation, forbidden line flux and remainder of the permitted line emission are produced in the bipolar lobes. Trammell et al. demonstrated that shock-excited emission dominates the spectra of the lobes of GL 618 with the emission indicative of shock velocities in the range of $50-100$ km s^{-1}. Long-slit optical spectroscopy of GL 618 suggests that the shock emission is associated with out-flowing gas (Carsenty and Solf 1982). Sanchez Contreras, Sahai, and Gil de Paz (2002) present a recent detailed ground-based spectroscopic study of GL 618. Their analysis of the emission line profiles and ratios suggest shock velocities in the range $75-200$ km s^{-1}. The largest velocities correspond to the tips of the bullets that we see in our HST images. Near-IR spectroscopy of GL 618 has revealed the presence of thermally excited H_2 emission (Thronson 1981; Latter et al. 1992). This object also exhibits [Fe II] emission thought to be associated with the shock-heated gas (Kelly, Latter, and Rieke 1992) and more recent observations establish that at least part of this emission is associated with an outflow (Kastner et al. 2001). Ueta, Fong, and

Meixner (2001) presented high spatial resolution near-IR images of GL 618 taken with the Subaru Telescope. The structure observed in the near-IR extends beyond the optical nebula and these images reveal the presence of "horns" and bullet-like structures associated with the bipolar lobes of GL 618. Ueta et al. suggest that the [Fe II] emission is associated with these features. These features are coincident with the tips of the outflows that we see in our HST images. These authors also found high velocity CO clumps at the positions of the IR bullets when they re-examined existing ^{12}CO J=1-0 interferometry data. Our new HST observations demonstrate that the source of the shock-excited emission in GL 618 is a set of highly collimated outflows originating in the central regions of the object.

2. Observations

We have obtained WFPC2 images of GL 618 as part of a HST Cycle 6 program. GL 618 was centered in the Planetary Camera which has a 36″x 36″field of view and a plate scale of 0.0455″pixel^{-1}. Images were obtained through three filters selected to isolate strong shock-excited emission lines, and thus trace the outflow in this source. The filters used were F631N (isolating [O I]λ6300 line emission), F656N (isolating Hα line emission), and F673N (isolating [S II] $\lambda\lambda$6717,31 line emission). In addition, we obtained images through F547M in an attempt to measure the adjacent continuum emission. The images of GL 618 were obtained on 23 October 1998 UT and exposure times ranged from 15 to 45 minutes. The images were processed through the HST data reduction pipeline procedures and cosmic rays were removed by combining several exposures of each object. The images were flux calibrated using the standard conversion to flux provided during the pipeline reduction procedures.

We have not removed the continuum from the narrow-band images that we present in this work. The F547M continuum band is contaminated by many weak emission lines making it impossible to reliably use images through this filter for continuum subtraction. Alternatively, we could have used an average value for the continuum derived from our ground-based work to remove continuum emission from our HST images. However, the line to continuum ratio is highly variable across the nebula making this approach unreliable. We point out that the continuum is approximately flat across the wavelength range covered by our narrow-band filters (as indicated in the ground-based spectroscopy, Trammell, Dinerstein, and Goodrich (1993)) and that this continuum is significantly weaker than the line emission in our ground-based spectroscopy (average line to continuum ratios of 50 to 125 for Hα, [S II], and [O I]). Further, the line emission seen in our HST images is concentrated in knot-like structures. In these regions of intense line emission, the line to continuum ratio is higher than the average values derived from the ground-based work. Consequently, the lack of continuum subtraction does not significantly affect our conclusions regarding the overall morphology of the shock-excited emission.

We have used our narrow-band images to form several line ratio maps for GL 618. The problems with continuum subtraction do introduce an additional error (approximately 10% in the worst case) into these maps. However, the primary purpose of these maps is to determine the outflow velocity. The outflow velocity is determined by comparing the observed line ratios with ratios predicted by models of shock-excited emission. The comparison with shock models results only in a range of possible shock velocities. The relatively small errors introduced into the line ratios by the lack of continuum subtraction do not significantly alter the value of the shock velocity that we derive.

3. Results And Analysis

Previous ground-based optical and near-IR work indicate that out-flowing gas is present in GL 618 (see section 1 for discussion). We present HST narrow-band imaging of GL 618 that confirm the presence of outflows in the lobes of this object and reveal the morphology of these flows. Figure 1 shows the 3-color image of GL 618 created by combining the Hα, [S II], and [O I] narrow-band images of this object. Figure 2 shows the individual narrow-band images. At least three distinct outflows are visible in each lobe of GL 618. The opening angles of these outflows are small, approximately 10 -15°. The central star is not visible in the HST images, consistent with previous optical and near-IR images (Latter et al. 1992).

A dust lane obscures the central star at optical wavelengths.

The morphologies seen in the [S II] and [O I] HST images are similar (see Figures 1 and 2). These images trace the morphology of the shock-excited emission in GL 618. The brightest emission occurs near the tip of each of the outflows and there is no forbidden line emission seen in the central regions of GL 618. Careful examination of the tip of the outflow labeled *a* in the west lobe of GL 618 (see Figure 1) reveals an excitation gradient across this region. Hα is brightest on the side of the knot that is facing away from the central regions of GL 618. This type of gradient is expected as material flowing away from the central source impinges on the surrounding nebular material. The bright spots at the tips of the outflows are not clumps of material being overrun by a wind or outflow (Trammell 2000). In this case, the brightest Hα emission would be present on the side of the bullet-like structures facing the central object. Based on their near-IR images and a reanalysis of high resolution CO data, Ueta, Fong, and Meixner (2001) also argue that the shock-excitation is produced when fast-moving material impacts the surrounding nebula.

The morphology observed in Hα differs from the forbidden line morphology. Hα emission is associated with the outflows, but in addition, a significant amount of Hα emission is seen towards the central regions of GL 618 (see Figures 1 and 2). Spectropolarimetric observations indicate that part of the Hα emission is reflected and part of this emission is produced by shocks in the lobes (Trammell, Dinerstein, and Goodrich 1993). We have spatially separated these components in the HST images. At least part of the Hα emission associated with the central regions of the object is probably reflected emission from an H II region buried deep in the nebula. Recent ground-based spectroscopy confirms that part of the Hα in the inner regions is scattered (Sanchez Contreras, Sahai, and Gil de Paz 2002). A high density H II region has been observed at the center of GL 618 at radio wavelengths (Kwok and Feldman 1981) and in the reflected optical spectrum (Trammell, Dinerstein, and Goodrich 1993). The Hα emission coincident with the outflows is the shock-excited component of the permitted line emission.

In addition to the Hα emission associated with the inner regions of the object and the outflows, a faint halo of emission is present in the Hα image (best seen in Figure 2 panel *a*). This faint halo is most likely Hα emission scattered by dust present in the outer regions of GL 618. GL 618 is known to be surrounded by an extensive molecular and dust envelope (see section 1 for discussion). The dusty material is probably part of the shell of material ejected by the central star of the object during its late AGB evolution. The axis of symmetry appears to be different for the scattered light envelope and the outflows seen in GL 618.

Three outflow features are seen in the images of GL 618. We believe that these features are the result of three separate outflows occurring simultaneously in GL 618. Alternatively, these features could be the result of one precessing jet. However, if this were the case we would expect to see S or spiral shaped morphology in the emission from the outflow (Cliffe et al. 1995; Livio, and Pringle 1996). We do not observe this type of morphology in the lobes of GL 618. We have further investigated the nature of the outflows by considering the recombination times of the ionized gas in the outflows. The presence of photoionized gas appears to be limited to the immediate vicinity of the central star in GL 618. This suggests that there is no significant source of ionization in the lobes of GL 618 other than that caused by thermal excitation in the outflows. If an outflow precesses away from a region, that region will continue to emit until the gas cools and recombines. Emission from S^+ is seen in all three outflow features. We can estimate the amount of time that the gas would continue to produce [S II] line emission after the outflow precesses away from a region by calculating the recombination time for S^+. The recombination time, τ_{recomb}, is given by

$$\tau_{recomb} = \frac{1}{N_e \alpha}$$

where N_e is the electron density and α is the recombination coefficient. The electron density is approximately 10^4 cm^{-3} based on ground-based spectroscopy (Trammell, Dinerstein, and Goodrich 1993) and the recombination coefficient for S^+ is 1.8 x 10^{-12} cm^3 s^{-1} (Arnaud and Rothenflug 1985, for T=10,000 K). The S^+ would recombine in approximately 1 year after the outflow moved away from a region. Based on this

result, we conclude that the three features seen in our HST images are three separate ongoing outflows. It has been suggested that simultaneous, multiple outflows have occurred or are occurring in several other young PN including the Starfish Twins (Sahai 2000), GL 2688 (Cox et al. 2000), Roberts 22 (Sahai et al. 1999), and the Frosty Leo Nebula (Sahai et al. 2000).

A ring-like morphology is seen in the outflows in all of the HST images (see Figure 1). This is most evident in the bright outflow labeled *b* in Figure 1. This morphology has not been seen in any ground-based images. The presence of these structures offers an opportunity to estimate the inclination of GL 618. Carsenty and Solf (1982) estimated the inclination of GL 618 be to 45°based on their optical spectroscopy. If GL 618 were viewed pole-on ($i = 90°$) we would expect the rings to be perfect circles. Instead, we see elliptical structures. We have estimated the inclination of three of the outflows based on the shapes of the rings as seen in the Hα and [S II] images. For the brightest outflow in the East lobe (labeled *b* in Figure 1), we estimate an inclination of 39°$\pm$ 4°. For the outflow labeled *c* in the East lobe, we estimate an inclination of 59°$\pm$ 10°. The feature labeled *d* in Figure 1 implies an inclination of 36°$\pm$ 4°. These results suggest that the outflows in GL 618 are not co-planar. These results also indicate that the previous estimate of the inclination of GL 618 was an overestimate. Sanchez Contreras, Sahai, and Gil de Paz (2002) also find a lower inclination for GL 618. Based on their spectroscopic observations of Hα in GL 618, these authors calculate an inclination angle of 24°$\pm$ 6°.

The ring-like features occur at semi-regular intervals along the outflows and could indicate that the source of the jet is episodic. Raga and Noriega-Crespo (1998) modeled this type of structure for episodic outflows associated with young stars. Alternatively, the rings could be the result of instabilities in the outflow. If the rings are the result of an episodic jet, we can estimate the amount of time between ejection events by looking at the spacing of the rings. The ring-like structures seen in outflow labeled *b* in Figure 1 are separated by approximately 0.5″. Assuming an outflow velocity of 120 km s^{-1} (see discussion later in this section) for the jet and a distance to GL 618 of 1.5 kpc, this implies an ejection event approximately every 35 years. Note that distance to GL 618 is uncertain and estimates range from 0.9 to 2 kpc (Schmidt and Cohen 1981; Goodrich 1991).

A dark arc is evident in the Hα image of the West lobe (see Figure 2a). This arc is located approximately 1.5″from the center of the dark lane. The dark arc is a region where there is a deficit of Hα emission. We believe that we are seeing dust in silhouette at the position of the dark arc. This dust could be located in the outer edge of the lane of dust obscuring the central star of GL 618. On the other hand, it could be a feature in the extended halo of GL 618. This halo is the remnant of AGB mass loss in this object. If the arc is a feature of the dust halo of GL 618, it might be similar to the arcs seen in HST images of GL 2688, another young planetary nebula. The arc structure in the extended scattered light halo of GL 2688 is explained as episodic mass loss by the star during the late AGB phase of evolution (Sahai et al. 1998b). A deep image of the scattered light halo of GL 618 could reveal if this type of episodic mass loss occurred in this object.

We have measured the average value of line ratios at the tips of the outflows labeled *a, b,* and *e* in Figure 1. These are the regions where outflowing material is impacting the surrounding nebula. In these regions [O I] / H$\alpha = 0.37 - 0.40$ and [S II]/H$\alpha = 0.11 - 0.16$. The values of the line ratios at the tips of the outflows provide an estimate of the shock velocity, and thus the outflow velocity in these regions. The bullet-like structures seen at the tips of the outflows have the geometry of bow shocks. Our estimates are an average of the line ratios across the entire bow shock region. Only the line ratios at the head of the bow shock, where the velocity component perpendicular to the shock is greatest, will reveal the maximum shock velocity. The rest of the bow shock consists of oblique shocks that result in line ratios indicative of lower shock speeds. Therefore, the shock velocity derived by examining line ratios from the entire region of the bow shock will provide an average value of the shock velocity. The outflow velocity at the tip of the outflow will be larger.

We have compared the observed line ratios with the models of thermally excited emission produced in a bow shock presented by Hartigan, Raymond, and Hartmann (1987). The line ratios are most consistent with their model of a bow shock with

velocity 100 km s^{-1}. If we compare our results to the planar shock models presented by Hartigan et al., we find that our observed line ratios are consistent with a shock velocity in the range of 40−100 km s^{-1}. Note that these models do not include the effects of magnetic fields. The field strength at the tips of the outflows is likely to be small so that this assumption is valid. However, if the field is strong ($\geq$ 300 μG) in these regions, we could be underestimating the shock velocity by 20−40 km s^{-1}.

The shock velocity is a measure of the relative speeds of the colliding gas. In the case of GL 618 an outflow is colliding with a surrounding shell of material that was ejected during the AGB/post-AGB phase. Meixner et al. (1998) have estimated an overall outflow velocity for the extended CO shell around GL 618 of 20 km s^{-1}. Assuming that the outflows are colliding with gas moving at approximately 20 km s^{-1}, the measured shock velocity (100 km s^{-1}) indicates a velocity for the collimated outflow to be about 120 km s^{-1} ($V_{outflow} = V_{shock} + V_{shell}$). This is consistent with estimates of the outflow velocity based on previous spectropolarimetry (Trammell, Dinerstein, and Goodrich 1993) and with optical and near-IR kinematic measurements (see section 1). This value is also consistent with the shock velocities recently reported by (Sanchez Contreras, Sahai, and Gil de Paz 2002).

Based on an outflow velocity of 120 km s^{-1} and assuming a distance to GL 618 of 1.5 kpc, we calculate the kinematic age of the outflows. The brightest outflows (labeled *a* and *b* in Figure 1) extend approximately 6″from the center of GL 618 in the HST images. We assume an inclination of 39°(see previous discussion). These parameters yield a kinematic age of $\lesssim$ 500 years for the outflows seen in the HST images. The outflows seen in GL 618 are a recent phenomenon and probably became active shortly after the star left the AGB.

Hajian, Phillips, and Terzian (1995) detected emission from CS in GL 618. This emission has an X-like morphology and is confined to the inner 4″of the object (this corresponds to the dark lane that we see in our optical images). The outflows that we see in the optical seem to be a continuation of the CS structure, as the optical outflows continue along a line extended from the CS structure. Meixner et al. (1998) examined the CO emission in GL 618 at high spatial resolution. The majority of the CO emitting gas in GL 618 is participating in a spherical expansion at 20 km s^{-1}. However, these high spatial resolution observations reveal that the halo of CO emission is not entirely spherically symmetric. The CO exhibits an X- like structure in the halo. This structure appears as 3 bright spots of CO emission located approximately 20″from the center of GL 618. These areas of low-velocity (20 km s^{-1}) CO emission are along the same axis as the CS and optical emission and are exterior to the optical outflows. The fact that the low-velocity CO emission related to the outflow is exterior to the optical emission is important. This indicates that the outflow is interacting with the neutral shell surrounding GL 618. Jets are playing a major role in the morphological development of this PN.

4. Discussion

Our observations demonstrate that emission from highly collimated outflows dominates the optical emission and morphology of GL 618. A comparison of the optical images with previous molecular line studies indicates that the jets are interacting with the neutral envelope surrounding GL 618. This interaction is shaping the neutral envelope of GL 618 and will determine the morphological evolution of this object. GL 618 is undergoing the early stages of PN development. Only a small region of photoionized gas is present in GL 618 and this ionized gas is found only in the immediate vicinity of the central star (Kwok and Feldman 1981). The fast wind described in the interacting winds model (Kwok, Purton, and Fitzgerald 1978) has not fully developed in GL 618. The interacting winds model suggests that it is the interaction of this fast wind with the surrounding neutral envelope that dictates the morphological evolution of a PN. In GL 618 the fast wind will be interacting with a neutral envelope that has already been significantly altered by the action of the jets.

The interaction of the jets with the neutral envelope seen in GL 618 is not unique. Recent observations of several other young PN indicate that jets may have a much more significant role in the overall development of these objects. CO observations of PN known to contain collimated outflows

have shown that these outflows are having a major impact on the surrounding neutral shells (Forveille et al. 1998; Cox et al. 2000; Huggins et al. 2000; Bachiller et al. 2000, e.g.). For example, in BD+30°3639 the CO observations reveal a pair of high velocity molecular knots just outside the ionized nebula. This is very similar to relationship between the molecular material and optical jets seen in GL 618. In all of these objects the jet's interaction with the neutral shell, not interacting winds, could be the dominant mechanism in determining the overall morphology of the PN.

The complex, multi-polar geometry observed in GL 618 is not unique. Sahai (2000) presented HST images of two young PN, He 2-47 and M1-37 (dubbed the Starfish Twins). These objects exhibit multi-polar morphology that is similar to that seen in GL 618. Sahai suggests that jets established the complex geometry of these nebulae. He estimates that the jets were active within the past few hundred years and suggests that multiple outflows occurred simultaneously in these objects. While the overall morphology of these objects is similar to GL 618, there are some differences. Knots or bullets of emission are prominent at the tips of the outflows in GL 618. These types of structures are not evident in the images of He 2-47 and M1-37. These bright spots mark the point where active jets collide with ambient material in GL 618. The jets are no longer active in the Starfish Twins so that the regions that correspond to tips have cooled significantly and do not appear as bright spots.

CO observations and HST imaging strongly suggest that jets play a important or dominant role in the shaping of some PN. These jets appear to be short-lived and they seem to operate during the post-AGB and/or PPN phases of evolution. Early jet action sets the stage for the complex morphologies we observed in some PN. High spatial resolution spectroscopy of these objects is needed to better understand the dynamics of the outflows and their impact of the surrounding material.

The overall morphology of the neutral envelope of GL 618, as traced by CO, is spherical (Meixner et al. 1998). The more recent mass outflows in this object are clearly aspherical. As is the case in other PN, the mass loss in GL 618 appears to have switched from spherical to aspherical soon after the star left the AGB. The kinematic age of the outflows suggest that the jets turned on sometime shortly after the star left the AGB. The trigger for the switch from spherical to aspherical mass loss in GL 618 appears to be the formation of collimated outflows in this object.

The debate concerning the origin of collimated outflows and also the formation of aspherical PN in general, centers on whether binary or single stars are responsible for producing aspherical mass loss. Both models of binary star interaction (Morris 1981; Soker and Livio 1994) and magnetic confinement (Garcia-Sergura 1997; Matt et al. 2000), while providing a scheme for producing the overall aspherical structure in PN, may also provide mechanisms to produce the highly collimated outflows. The complex, multi-polar outflow geometry seen in GL 618 may be difficult for either of these types of models to explain.

The authors thank the referee for useful comments and suggestions. This work was supported by NASA through grant number GO-06761 from the Space Telescope Science Institute, which is operated by AURA, Inc., under NASA contract NAS 5-26555.

REFERENCES

Arnaud, M. and Rothenflug, R. 1985, A&AS, 60, 425

Bachiller, R., Forveille, T., Huggins, P. J., Cox, P., and Maillard, J. P. 2000, A&A, 353, L5

Balick, B. 1987, AJ, 94, 671

Carsenty, U. and Solf, J. 1982, A&A, 106, 307

Cliffe, J. A., Frank, A., Livio, M., and Jones, T. W. 1995, ApJ, 447, L49

Cox, P., Lucus, R., Huggins, P. J., Forveille, T., Bachiller, R., Guilloteau, S., Maillard, J. P., and Omont, A. 2000, A&A, 353, L25

Dayal, A., Hoffmann, W. F., Beiging, J. H., Hora, J. L., Deutsch, L. K., and Fazio, G. G. 1998, ApJ, 492, 603

Dwarkadas, V. V., Chevalier, R. A., and Blondin, J. M. 1996, ApJ, 457, 773

Forveille, T., Huggins, P. J., Bachiller, R., and Cox, P. 1998, ApJ, 495, L111

Frank, A. 1994, AJ, 107, 261

Garcia-Sergura, G. 1997, ApJ, 489, L189

Goodrich, R. W. 1991, ApJ, 376, 654

Greig, W. E. 1971, A&A, 10, 161

Hajian, A. R., Phillips, J. A., and Terzian, Y. 1995, ApJ, 446, 244

Hartigan, P., Raymond, J., and Hartmann, L. 1987, ApJ, 316, 323

Huggins, P. J., Forveille, T., Bachiller, R., and Cox, P. 2000, ApJ, 544, 889

Icke, V., Balick, B., and Frank, A. 1992, A&A, 253, 224

Kastner, J. H., Weintraub, D. A., Gatley, I., and Henn, L. A. 2001, ApJ, 546, 279

Kastner, J. H., Soker, N., and Rappaport, S., eds. 2000, APS Conference Series 199, Asymmetrical Planetary Nebulae II: From Origins to Microstructures (San Francisco: ASP)

Kelly, D. M., Latter, W. B., and Rieke, G. H. 1992, ApJ, 395, 174

Khan, F. D. and West, K. A. 1985, MNRAS, 212, 837

Kwok, S., Su, K. Y. L., and Hrivnak, B. J. 1998, ApJ, 501, L117

Kwok, S. and Feldman, P. A. 1981, ApJ, 247, L67

Kwok, S., Purton, C. R., and Fitzgerald, P. M. 1978, ApJ, 219, L125

Latter, W. B., Maloney, P. R., Kelly, D. M., Black, J. H., Rieke, G. H., and Rieke, M. J. 1992, ApJ, 389, 347

Livio, M. and Pringle, J. E. 1996, ApJ, 465, L55

Manchado, A., Guerrero, M. A., Stanghellini, L., and Serra-Ricart, M. 1996, The IAC Morphological Catalog of Northern Galactic Planetary Nebulae (La Laguna, Spain: Instituto de Astrofisica de Canarias)

Matt, S., Balick, B., Winglee, R., and Goodson, A. 2000, ApJ, 545, 965

Meixner, M., Campbell, M. T., Welch, W. J., and Likkel, L. 1998, ApJ, 509, 392

Meixner, M., Skinner, C. J., Graham, J. R., Keto, E., Jernigan, J. G., and Arens, J. F. 1997, ApJ, 482, 897

Morris, M. 1981, ApJ, 249, 572

Neri, R., Kahane, C., Lucus, R., Bujarrabal, V., and Loup, C. 1998, A&AS, 130, 1

Raga, A. and Noriega-Crespo, A. 1998, AJ, 116, 2943

Sahai, R. 2000, ApJ, 537, L43

Sahai, R. and Trauger, J. T. 1998a, AJ, 116, 1357

Sahai, R. et al. 1998b, ApJ, 493, 301

Sahai, R., Zijlstra, A., Bujarrabal, V., and te Lintel Hekkert, P. 1999, AJ, 117, 1408

Sahai, R., Bujarrabal, V., Castro-Carrizo, A., and Zijlstra, A. 2000, A&A, 360, L9

Sanchez Contreras, C., Sahai, R., and Gil de Paz, A. 2002, ApJ, in press

Schmidt, G. D. and Cohen, M. 1981, ApJ, 246, 444

Schwarz, H. E., Corradi, R. L. M., and Melnick, J. 1992, A&AS, 96, 23

Speck, A. K., Meixner, M., and Knapp, G. R. 2000, ApJ, 545, L145

Soker, N. and Livio, M. 1994, ApJ, 421, 219

Soker, N. and Livio, M. 1989, ApJ, 339, 268

Thronson, H. A. 1981, ApJ, 248, 984

Trammell, S. R. 2000, in APS Conference Series 199, Asymmetrical Planetary Nebulae II: From Origins to Microstructures (San Francisco: ASP) 147

Trammell, S. R., Dinerstein, H. L., and Goodrich, R. W.1994, AJ, 108, 984

Trammell, S. R., Dinerstein, H. L., and Goodrich, R. W. 1993, ApJ, 402, 249

Ueta, T., Fong, D., and Meixner, M. 2001, ApJ, 557, L117

Ueta, T., Meixner, M., and Bobrowsky, M. 2000, ApJ, 528, 861

Zuckerman, B. and Aller, L. H. 1986, ApJ, 301, 772

AAS LaTeX macros v5.0.

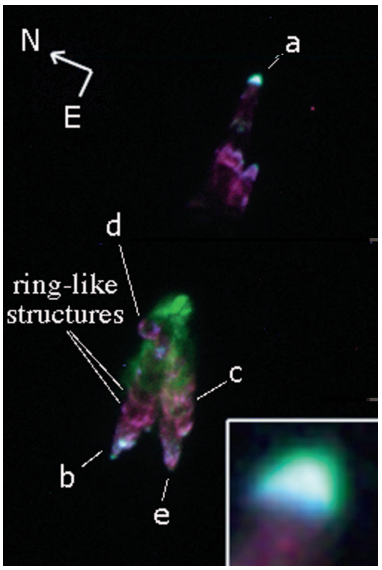

Fig. 1.— Combination of three narrow-band WFPC2 images of GL 618. In this figure green represents the Hα emission, blue the [O I] emission and red the [S II] emission. The forbidden line emission is concentrated in three distinct collimated outflows that originate in the central regions of GL 618. The Hα emission is found in the outflows and components of this emission are also present closer to the central dark lane of the object and in in an extended halo. The size of this image is approximately 12″x 17″. The insert displays a detailed view of the outflow labeled *a*.

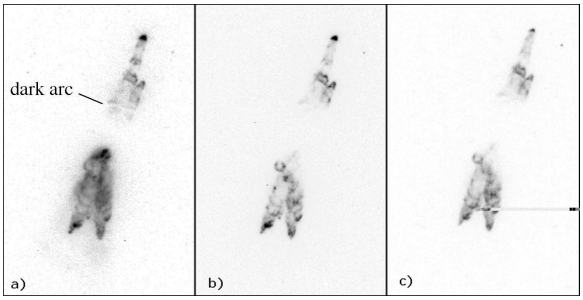

Fig. 2.— (a) The F656N filter image which traces the Hα emission in GL 618. Notice the extended halo and the dark arc. (b) The F631N filter image which traces the [O I] emission (c) The F673N filter image which traces the [S II] emission. The size of each image is approximately 12″x 17″.